

Iodide interaction with natural pyrite

Laure Aimoz · Enzo Curti · Urs Mäder

Received: 25 November 2010 / Published online: 4 January 2011
© Akadémiai Kiadó, Budapest, Hungary 2011

Abstract ^{129}I is one of the major dose-determining nuclides in the safety analysis of deep storage of radioactive waste. Iodine forms anionic species that hardly sorb on the surfaces of common host-rock minerals. Recently, interest has arisen on the role of pyrite, an accessory mineral capable of binding anionic selenium. Whereas the interaction of selenium with pyrite is well documented, corresponding results on iodine sorption are still scarce and controversial. Pyrite is present in argillaceous rocks which are being considered in many countries as potential host rocks for a radioactive waste repository. The uptake of iodide (I^-) on natural pyrite was investigated under nearly anoxic conditions ($\text{O}_2 < 5$ ppm) over a wide concentration range (10^{-11} – 10^{-3} M total I^-) using ^{125}I as the radioactive tracer. Weak but measurable sorption was observed; distribution coefficients (R_d) were less than $0.002 \text{ m}^3 \text{ kg}^{-1}$ and decreased with increasing total iodide concentration. Iodide sorption was connected to the presence of oxidized clusters on the pyrite surface, which were presumably formed by reaction with limited amounts of dissolved oxygen. The results obtained indicated that pyrite cannot be considered as an effective scavenger of ^{129}I under the geochemical conditions prevailing in underground radioactive waste geologic storage.

Electronic supplementary material The online version of this article (doi:10.1007/s10967-010-0959-9) contains supplementary material, which is available to authorized users.

L. Aimoz · E. Curti
Laboratory for Waste Management, Paul Scherrer Institut, 5232
Villigen PSI, Switzerland

L. Aimoz (✉) · U. Mäder
Institute of Geological Sciences, University of Bern,
Baltzerstrasse 1-3, 3012 Bern, Switzerland
e-mail: laure.aimoz@psi.ch

Keywords FeS_2 · Iodide · Sorption · Surface oxidation · I-129

Introduction

Aqueous corrosion of nuclear waste planned to be disposed of in radioactive waste repositories will release long-lived radionuclides, including ^{129}I . In the current Swiss geologic storage concepts [1], ^{129}I will be released predominantly from spent fuel, either as iodide (I^-) or iodine ($\text{I}_2(\text{g})$). ^{129}I accumulates on fuel grain boundaries and in the fission gas. Upon the failure of the metallic containers foreseen to contain radioactive waste, a sudden release pulse of radionuclides will occur (“instant release fraction”) [1, 2]. Anionic species such as I^- do not sorb significantly on the surfaces of major minerals in the repository near-field (e.g. clays, other silicates, sulfates), since their surfaces are negatively charged under the neutral to alkaline pHs prevailing in such environments [1]. ^{129}I is therefore considered to be mobile compared with fission products and actinides dissolved as cationic species. Natural iodine in clay formations was found to be associated with carbonate minerals [3] having both biogenic and inorganic origin. Although the radioiodine released from the waste could potentially be trapped by carbonate minerals via isotopic exchange, this mechanism is judged by the authors to be ineffective on the short term due to the inaccessibility of the natural iodine in the carbonate mineral lattice (low solid state diffusion coefficients). This implies that uptake of radioiodine by carbonate minerals could only proceed by surface adsorption, and will be limited by the small specific surface area of carbonate minerals. Due to the combined effect of the long half-life (1.57×10^7 years for ^{129}I) and low retention capacity, this fission product is among the

major dose-determining nuclides in the safety analysis of radioactive waste geologic storage [1]. In the context of performance assessment, compacted bentonite will be used as the backfilling material for sealing the repository tunnels of the foreseen Swiss radioactive waste repository. So far, R_d values for iodine on bentonite were considered to be low, about $5 \times 10^{-4} \text{ m}^3 \text{ kg}^{-1}$ ($3 \times 10^{-5} \text{ m}^3 \text{ kg}^{-1}$ in Opalinus Clay) [1]. Diffusion experiments with Avonlea bentonite also showed that iodine could be considered as a non-sorbing species [4].

Pyrite is a minor mineral occurring in small amounts (about 0.3 wt%) in Wyoming bentonite MX-80, the reference material currently considered for sealing the tunnels of the planned high-level radioactive waste repository in Switzerland. It is also ubiquitous in the Opalinus clay host formation (about 1 wt%) [1]. Surface potential measurements for the pyrite surface yielded points of zero charge in the acidic region, $\text{pH}_{\text{pzc}} \sim 1.7\text{--}2.4$ [5, 6] when carried out under controlled anoxic conditions. According to these data, the pyrite surface is expected to be negatively charged in the pH-region of natural waters, therefore electrostatic binding of cations such as Am^{3+} may occur [7], whereas no electrostatic binding of anionic species like I^- or IO_3^- should occur. A second group of measurements [8] was conducted under oxidizing conditions and indicates much higher values, $\text{pH}_{\text{pzc}} \sim 6.4\text{--}7$. These values are intermediate between the low pH_{pzc} determined for non-oxidized pyrite and those ($\text{pH}_{\text{pzc}} > 8$) of ferric oxides [9]. Pyrite surfaces strongly tend to oxidize once they are exposed to air. ^{129}I is dominantly anionic in natural aqueous solutions, both under reducing and oxidizing conditions (I^- or IO_3^-). Therefore, pyrite is not expected to have a significant sorption capacity for iodine in geological environments, unless non-electrostatic binding mechanisms play a role.

To date, the few experimental studies on iodide sorption onto pyrite have yielded contradictory results. A summary of the published data is presented in Table 1. The results from earlier investigations suggested high sorption values for iodide onto pyrite. Fuhrmann et al. [10] and Strickert et al. [11] claimed that up to $\sim 100\%$ of the iodide radiotracer used in their experiments was sorbed on pyrite. Zhuang et al. [12] also showed up to 22.8% iodide uptake at low iodine concentration ($\sim 10^{-13} \text{ M}$). These three studies were based on experiments carried out with natural pyrite samples without any surface pre-treatment, at low iodide concentrations ($< 10^{-10} \text{ M}$) and open to the air. In order to explain the high degree of iodide uptake, Strickert et al. [11] suggested incorporation into the crystal lattice. Fuhrmann et al. [10] interpreted the high sorption values for iodide as being a possible consequence of pyrite surface oxidation based on X-Ray Absorption Near-Edge Spectroscopy (XANES) measurements. Fuhrmann et al. [10] claimed that oxidation produced a coating of ferric oxides;

in the meantime, sulfuric acid formed and acidified the solution to pH 4. Since ferric oxides have a point of zero charge (pH_{pzc}) above 8 [9], the dissolved iodide could have sorbed onto the positively charged surface of the ferric oxides coating.

In recent studies carried out under anoxic conditions iodide sorption onto pyrite was not detectable at high total dissolved iodine concentrations ($10^{-4}\text{--}10^{-2} \text{ M}$) [13, 14]. However, Kaufhold et al. [13] and Naveau et al. [14] could not exclude that strong iodide sorption could occur at lower levels of total iodine in aqueous solution. This study aims at giving an unequivocal answer by investigating iodide uptake on pyrite over a wide range of concentrations ($10^{-11}\text{--}10^{-3} \text{ M}$ total I) under nearly anoxic conditions.

Retention studies of iodide on argillaceous host rocks being considered for nuclear waste deep storage were carried out on the Boda claystone formation [15] (Hungary), the Opalinus clay [16] (Switzerland), and on the Callovian–Oxfordian clay [17] (France). The results presented in these papers all indicated a very limited retardation of iodine, although the Opalinus clay and the Callovian–Oxfordian clay are reported to contain on average $\sim 1\%$ pyrite. These results therefore seem to indicate that pyrite does not play a major role on the retention of iodide under repository conditions. With this study we attempt to resolve the contradictory results so far available in the literature by investigating iodide sorption on pyrite under carefully controlled experimental conditions.

Materials and methods

Mineral preparation

The use of natural pyrite was preferred due to the complex synthesis procedures required for obtaining pure pyrite ($\alpha\text{-FeS}_2$) free of other Fe_xS_y sulfides [18, 19]. Selected natural pyrite samples from two separate mines (Huanzala, Peru and Navajun, Spain) were purchased from Ward's Natural Science, Rochester, NY. The Huanzala ore is a Zn–Pb strata-bound hydrothermal deposit hosted in a Cretaceous limestone formation in which the pyrite formation occurred in the early stages of mineralization as fine-grained to coarse-grained granular masses [20]. The Navajun ore, hosted in a Jurassic marl formation, is characterized by euhedral cm to dm sized cubic pyrite crystals. The widespread occurrence of chloritoid inclusions in the pyrite crystals [21] points to a metamorphic origin (greenschist facies). X-Ray powder diffraction patterns of samples from both sites were recorded on a Phillips Xpert-Pro diffractometer (CuK_α radiation, 2θ from 5 to 70°) and confirmed pyrite as the only detectable crystalline phase.

Table 1 Summary of iodide sorption studies onto pyrite

Ref.	Pyrite origin	O ₂ exclusion	Particle size (μm)	S/L (g L ⁻¹)	Starting solution	Reaction time (days)	pH	[I] range (mol L ⁻¹)	% Sorbed	R _d (m ³ kg ⁻¹)
[11]	Natural mineral, unknown origin	No	150–250	500–1000	H ₂ O	4	Free	~10 ⁻¹⁰	~100 ^a	0.3–3
[10]	Huanzala, Peru	No	<180	25	H ₂ O	1–15	8.7	~10 ⁻¹⁴	82 to ~100	0.18–4.0 ^a
[12]	China	No	125–250	50	H ₂ O	21	Free	~10 ⁻¹³	22.8	0.006 ^a
[13]	Synthetic HNO ₃ washed	Yes	<50	8	NaClO ₄ 0.05 M	0.25–5	2–12	10 ⁻⁴	Insign.	–
[14]	Norway and Germany	Yes	<125	10	H ₂ O	2	Free or 10	10 ⁻²	<LD	–
This study	Huanzala, Peru	Yes	<63	50	H ₂ O	7	Free	~10 ⁻³	<LD	–
								~10 ⁻⁶	3.0	0.0006
								~10 ⁻¹¹	<LD	0.002
								~10 ⁻³	0	–
								~10 ⁻⁶	2.6	0.0005
Navajun, Spain HCl washed	Yes	<63	50	H ₂ O	7	Free	~10 ⁻³	0	–	
							~10 ⁻⁶	2.6	0.0005	
							~10 ⁻¹¹	6.5	0.001	
								~10 ⁻¹¹	6.2	0.001

Insign. insignificant, *LD* limit of detection

^a Calculated here for comparison

Due to the sensitivity of pyrite towards surface oxidation [19, 22], special care was taken in the preparation of pyrite before carrying out the iodine sorption experiments under anoxic conditions. The adopted procedures followed those given in Moses et al. [19], which were assessed to be the most effective way for limiting oxidation artifacts, and were performed in a glove box (N₂ atmosphere; O₂ < 5 ppm), except for crushing and centrifugation. For the ¹²⁵I sorption experiments, Huanzala and Navajun pyrite fragments were crushed in acetone to a fine-grained powder in a tungsten carbide mill in order to enhance surface reactivity. The powdered pyrite samples were passed through a 63 μm sieve. The fraction below 63 μm was thoroughly washed in 12 M HCl (reagent grade, Merck) to dissolve any possible secondary oxides on the surfaces. Samples were then rinsed several times with degassed ethanol, and eventually dried by evaporation at room temperature in the glove box. Specific surface areas of the powdered fractions below 63 μm were measured by Brunner Emmet Teller (BET) method under N₂ atmosphere. The sieved Huanzala pyrite and the Navajun pyrite used for the experiments had specific surface areas of 0.94 and 0.46 m²/g respectively.

Quantitative iodine sorption experiments

The Milli-Q[®] water used for preparing the solutions was degassed during 1 h with N₂ to purge dissolved O₂. A non-complexing buffer from the Good's series, HEPES (Sigma-

Aldrich) was used together with NaOH (Merck, analytical grade) for the pH-controlled experiments [23]. ¹²⁵I (prevalently as iodide) radiotracer (γ-emitter, half-life 59.4 days) dissolved in a slightly alkaline solution was purchased from Amersham International Ltd. Potassium iodide (KI analytical grade, Merck) containing only stable ¹²⁷I was used to prepare a 0.1 M KI solution.

The pyrite powder was added to the aqueous solution at various solid to liquid ratios ($S/L = 5\text{--}50\text{ g L}^{-1}$) in 50 mL vials. The suspensions were then spiked with an appropriate amount of ¹²⁵I and when necessary, with a 0.1 M KI solution to increase the total iodine concentration to the required value. The solid was then maintained in suspension on an end-over-end shaker for 7 days.

After 7 days, the suspension was either filtered through 0.45 μm acetate cellulose filters (Fisherbrand) or centrifuged at 95,000×g (max) for 60 min. The cut-off size in the centrifugation process is equivalent to 0.05 μm [24]. The final pH values were measured with a combined glass electrode (Metrohm). The ¹²⁵I activities of supernatant solutions (after centrifugation), or filtrates, were radio assayed in duplicate in a gamma-counter (γ-counter Cobra, Canberra-Packard) together with standard solutions, and then recalculated at the sampling time (t_0). From the activity measurements of sample and standard solutions, the extent of iodide sorption on pyrite could be determined. The fraction of iodide sorbed, F (%) and the distribution coefficient, R_d (m³ kg⁻¹) were determined from the following equations:

$$F = \left(1 - \frac{A_{\text{sple}}}{A_{\text{std}}}\right) \quad (1)$$

$$R_d = \left(\frac{F}{1-F}\right) \times \frac{V}{m} \quad (2)$$

where A_{sple} (Bq) is the ^{125}I activity remaining in the filtrate or in the supernatant after centrifugation at the sampling time; A_{std} (Bq) is the standard activity, corresponding to the total ^{125}I activity initially added to the suspension; V (m^3) is the volume of aqueous solution and m (kg) is the mass of solid sample. Overall uncertainties were calculated according to classical error propagation theory [25].

Blank experiments conducted without pyrite indicated no detectable iodide sorption on the sample bottle walls, the filters, and the centrifuge tube walls.

Results

^{125}I tracer experiments

Iodide uptake experiments conducted at a solid to liquid ratio (S/L) of 5 g L^{-1} resulted in no difference (below 1% difference) of ^{125}I measured in the standards and the sample. Subsequent experiments were therefore conducted at higher pyrite loadings ($\sim 50 \text{ g L}^{-1}$), in order to increase the sorbed quantities of ^{125}I in the samples. The results discussed hereafter refer to such high S/L ratios.

The uptake of iodide on both samples of pyrite was first investigated at low concentration (using the ^{125}I tracer only), without pH buffering. In this set of experiments, the pH decreased from near-neutral to slightly acidic (pH 4–5). Acidification during pyrite weathering is a well-known phenomenon. It occurs even under anoxic conditions since only a very small O_2 contamination is sufficient to oxidize small amounts of sulfide on the pyrite surface and release it as sulfuric acid [26, 27]. In addition, we cannot exclude a contribution from traces of acid remaining from the surface washing. After 7 days, two aliquots of well-agitated suspension were collected. The first one was centrifuged (cut-off size = $0.05 \mu\text{m}$), and the second one was filtered through $0.45 \mu\text{m}$ in order to detect the amount of iodide sorbed on colloids (0.05 – $0.45 \mu\text{m}$ fraction). Within experimental uncertainties, comparable results were obtained for both pyrites, revealing a limited but significant sorption of the iodide tracer (Fig. 1). The percentage sorbed was always within ~ 2 – 10% of the total added iodide. Approximately one-third could be assigned to uptake by colloids passing through the filter, but separated from the solution after centrifugation (0.05 – $0.45 \mu\text{m}$ fraction).

Smaller R_d values than previously reported in the literature were determined in our experiments (Fig. 2), notably

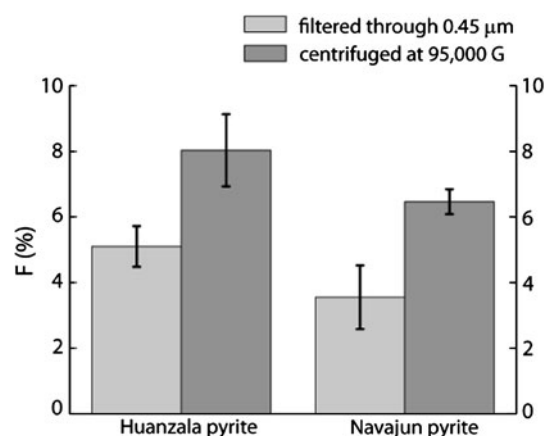


Fig. 1 F , percentage of I^- sorbed at 10^{-11} M total iodide added in solution, in pure water for Navajun and Huanzala pyrites

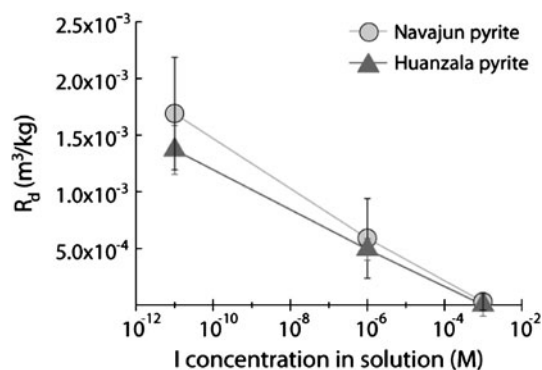


Fig. 2 R_d values for iodide sorption on pyrite, in pure water under anoxic conditions. Circles pyrite from Navajun, triangles pyrite from Huanzala

for the Huanzala pyrite, which has the same origin as the pyrite used by Fuhrmann et al. [10]. For the Huanzala pyrite, some experiments were repeated using different batches of pyrite powder. All four replicates yielded similar results, except for a single outlier showing a higher sorption with $F = 60.9\%$ ($\pm 0.7\%$, 2σ) after centrifugation. This result is considered an artifact but remains unexplained.

In order to understand the dependence of sorption on the dissolved iodide concentration, distribution coefficients (R_d) were determined after centrifugation for both pyrites and including iodide concentrations ranging from 10^{-11} – 10^{-3} M . A decrease of R_d with increasing iodine concentration was observed, yielding a non-linear isotherm. R_d decreased from $\sim 1.5 \times 10^{-3} \text{ m}^3 \text{ kg}^{-1}$ at 10^{-11} M I to $\sim 5 \times 10^{-4} \text{ m}^3 \text{ kg}^{-1}$ at 10^{-6} M I . At 10^{-3} M I the R_d cannot be calculated because no differences could be detected between the standard and sample concentration.

Finally, the influence of pH and E_h on iodide uptake was investigated by carrying out two sets of additional experiments: (i) with buffered pH in the glove box, and (ii) with

unbuffered pH under air atmosphere (Table 2). The tests in air were carried out at low iodide concentration (tracer only) with Navajun pyrite previously washed in the glove box, but without any special care taken to prevent an exposure of the pyrite surface to dissolved oxygen. For this purpose our experiments were carried out with non-degassed Milli-Q outside the glove box. The buffered pH experiments in the glove box were carried out using non-complexing HEPES buffer and NaOH to maintain pH ~ 8 , which is comparable to the pH expected in the high-level radioactive waste repository foreseen in Switzerland [28].

Under anoxic conditions, no noticeable difference was observed between the results obtained with unconstrained (free-drift) pH, and the corresponding experiment buffered at pH 8. For the experiment open to the air, a drop by two units to \sim pH 3 was observed. A weaker iodide uptake was observed at this pH.

As already mentioned, oxidation of pyrite in aqueous media is frequently observed even in laboratory tests performed at trace levels of O₂ [26, 27]. In our batch experiments, a partial oxidation of the pyrite surface could also not be avoided, as indicated by the observed moderate drop in pH. In order to interpret the sorption data, we assessed the maximum amount of oxidized pyrite following the oxidation rate equation (Eq. 3) proposed by Williamson and Rimstidt [27], who also used an acid-leached natural pyrite for their kinetic experiments:

$$r = 10^{-8.19} \frac{\text{DO}^{0.5}}{[\text{H}^+]^{0.11}} \quad (3)$$

where r is the oxidation rate in mol m⁻² s⁻¹, DO the concentration of dissolved oxygen in mol L⁻¹ and [H⁺] the free proton concentration in mol L⁻¹. The amount of dissolved oxygen was calculated (i) based on Henry's Law using a constant for oxygen gas–water equilibrium at 25 °C equal to 2.293×10^{-5} [29] and (ii) as a maximum remaining O₂ concentration in the degassed solutions as estimated by Butler et al. [30]. Complete equilibration with the gas phase in the glove box (2 m³, 5 ppm O₂) would yield a DO concentration of $\sim 10^{-8}$ M. Butler et al. [30] investigated the efficiency of a degassing procedure similar to the one used in our experiments, by monitoring the decrease of DO concentration in water against purging times with high-purity N₂. They measured a minimum

Table 2 Influence of pH and oxidation conditions on the iodine uptake at 10^{-11} M I⁻ onto the Navajun pyrite

	pH	F (%)	2σ
Pure water, glove box	5.1	6.46	0.38
Buffered water, glove box	8	6.23	0.16
Pure water, open to the air	3.3	1.18	0.42

Table 3 Maximum assessed percentage of oxidized surface of the pyrite for experiments in the glove box and open to the air

O ₂ in the gas phase	DO (M)	pH	Oxidized surface (%)
Glove box, 5 ppm	6×10^{-6}	5.1	0.40
Air, 20%	2.4×10^{-4}	3.3	1.59

residual DO in water after purging N₂ during 1 h of $\sim 6 \times 10^{-6}$ M. Longer purging times did not lower this concentration. Therefore, we cannot exclude that our degassed solutions contained similar DO concentrations. This value of DO = 6×10^{-6} M was much larger than complete equilibration with the gas phase in the glove box and was taken as an upper limit for our glove-box experiments. For the experiments open to the air, where the Milli-Q[®] water was not degassed, we assumed a DO concentration in equilibrium with air, DO $\sim 2 \times 10^{-4}$ M. Taking into account the BET measurements of our pyrite samples, the measured pH, and using Eq. 3, the maximum percentage of oxidized surface was estimated to be less than 2% for both types of experiments (Table 3).

Pourbaix diagrams

In order to facilitate the interpretation of the results, Pourbaix diagrams were generated using the software PhreePlot (beta version, <http://www.phreeplot.org/>), which is based on the geochemical speciation and solid phase saturation model of PHREEQC (Fig. 3). Total S and Fe concentrations were fixed at values approaching those relevant for our systems. Thermodynamic data for iron and sulfur species were taken from the Nagra-PSI database [31]. Thermodynamic data for iodine were selected from [32] and [29] in order to obtain a set of equilibrium constants for the most common species, including aqueous (I₂, I₃⁻, IO₃⁻, IO₄⁻, IO⁻, HIO, HIO₃), solid (I₂) and gaseous (I₂) phases. In order to make the interpretation easier, the stability field of pyrite was superimposed on the Eh–pH diagram for iodine (Fig. 3b). Even though only the Pourbaix diagram for 10^{-6} M I⁻ is shown in Fig. 3b, calculations for higher and lower concentrations did not change the stability relationships.

Discussion

Thermodynamic stability

Even for the experiments open to the air, carried out using non-degassed water, the calculated maximum oxidized fraction was low (1.6%), but larger than the one calculated for the pyrite treated under “anoxic” conditions (0.4%). For the experiments open to the air the measured final pH

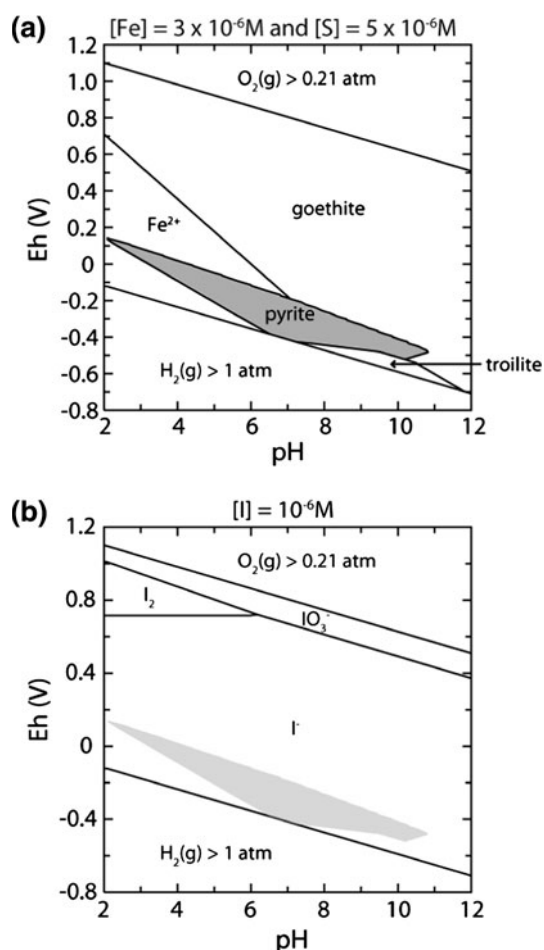


Fig. 3 Eh-pH diagrams at 25 °C for **a** the S-Fe-O-H system with total Fe = 3×10^{-6} M and total S = 5×10^{-6} M, **b** I-O-H with total I = 10^{-6} M. On figure **b** the stability field of pyrite from **a** is superimposed as shaded areas

was considerably lower than for the “anoxic” experiments (pH 3.3 vs. pH 5.1), suggesting, as expected, a more extensive oxidation of the pyrite surface owing to the larger amount of available oxygen, compared to the analogous experiment conducted in the glove box.

However, in both types of experiments, only a very limited fraction of the exposed pyrite surface (upper limit of 2%) was calculated to be affected by the oxidation process. Thus, despite the thermodynamic disequilibrium between gas and solid phase, the amount of oxidant (DO) available in solution was really insufficient to consume the large amount of reduced S and Fe on the pyrite surface. In the case of the glove box experiments, the oxidation reaction proceeds until total consumption of the limited dissolved oxygen present, leaving behind a large excess of pyrite in thermodynamic equilibrium with the rest of the system. Therefore, at the end of the reaction, the oxidation potential must have been buffered within the stability field

of pyrite (e.g. Eh -0.2 to 0.0 V at pH ~ 5 , see Fig. 3a). As shown in Fig. 3b, under such conditions the stable form of iodine is iodide (I^-). Consequently, one can exclude I^- oxidation to I_2 or IO_3^- species across the entire pH and concentration range of the experiments (from 10^{-11} to 10^{-3} M I^- and pH ~ 3 to pH ~ 8), except perhaps in the limited oxidized regions, as also mentioned by Fuhrmann et al. [10].

Iodide sorption

The uptake of iodide was found to be similar for both natural pyrites investigated in the present study (Fig. 2). The sorbed fractions systematically decreased with increasing iodide concentration and were only measurable at low iodide concentrations (10^{-11} and 10^{-6} M I^-). At higher concentrations (10^{-3} M) no uptake was measurable. Kaufhold et al. [13] and Naveau et al. [14] did also not observe iodide sorption onto pyrite at comparably high concentrations (10^{-4} – 10^{-2} M I^-). These authors argued that significant iodide uptake may be possible at very low iodide concentration. Our results confirmed this prediction, a weak but measurable iodide uptake by pyrite was observed at total iodide concentrations in the picomolar to micromolar region. In addition, a significant proportion (approximately one-third) of the sorbed iodide was demonstrated to be taken up by colloidal particles. We attributed this phenomenon to the higher specific surface area of such colloids compared to the micrometer-sized particles.

Surface oxidation

As discussed earlier, the presence of small regions of oxidized pyrite surface may be assumed. The pyrite oxidation process generates soluble sulfate ions, whereas Fe^{2+} ions are oxidized to insoluble Fe(III) species. Therefore, the assumed oxidized regions on the pyrite surface are probably very similar to the Fe(III) oxides which precipitate on the pyrite surface after an extensive oxidation reaction with dissolved O_2 [26, 33]. For the whole set of experiments, the pH varied between 3.3 and 8. This pH range is above the potential of zero charge (pH_{pzc}) of non-oxidized pyrite (>1.7 – 2.4) [5, 6] but below the pH_{pzc} of Fe(III) oxides (<8) [9], which implies a negative surface charge for the predominantly non-oxidized part of the pyrite and a positive surface charge for the limited oxidized fraction. Outer-sphere complexation of iodide on the non-oxidized regions of the pyrite samples can therefore be excluded, but it could be possible on the “Fe(III) oxide-like” areas.

At first glance, this explanation seems to contradict our experimental data. The smallest fraction of sorbed iodide

was only found in the experiments open to the air (Table 3), for which the estimated oxidized surface was much larger than for experiments carried out in the glove box. This apparent inconsistency could be resolved by considering the thermodynamic stability of Fe(III)-oxides as a function of pH. Indeed, thermodynamic data indicate that Fe(III) oxides are not stable under acidic conditions and tend to dissolve below pH 4 [34]. Even if more extensive oxidation did occur in the open to the air experiments, the oxidized surface may continuously dissolve at a pH below 4. Such a behavior was also indicated by the Pourbaix diagram for the Fe–S–O–H system (Fig. 3a) showing that goethite becomes unstable at low pH. The overall effect would paradoxically be a greater amount of oxidized surface in the experiments carried out under nearly anoxic conditions compared to the experiments open to the air, and consequently a larger quantity of sorbed iodide under nearly anoxic conditions. We therefore concluded that weaker iodide uptake observed in the experiments open to air does not contradict the hypothesis of iodide being bound to Fe(III) oxide-like clusters on the pyrite surface.

Unlike Strickert et al. [11] and Fuhrmann et al. [10], digestion of possible pre-oxidized surface was taken care of in the present work by leaching our powdered samples with concentrated HCl prior to each sorption experiment. The inability of eliminating such artifacts could explain the high R_d values obtained at pH above 4 by Strickert et al. [11] and Fuhrmann et al. [10]. An extensive mineral surface oxidation prior to sorption experiments and/or the presence of oxidized inclusions within their natural pyrite could conceivably be the origin of the larger uptake observed by these authors.

In conclusion, our results suggest that the uptake of iodide by pyrite is related to the formation of oxidized domains on the mineral surface formed after reaction with dissolved oxygen. Even trace amounts of dissolved oxygen are sufficient to explain the observed iodide sorption in the picomolar concentration range. The underlying assumption in this model is that I sorption is exclusively due to electrostatic outer-sphere complexation. However, the exact uptake mechanism is still not fully understood. We cannot exclude that other binding mechanisms (e.g. covalent bonds, attachment to surface defects) also play a role. Unfortunately, at such low concentrations spectroscopic methods are not sufficiently sensitive to experimentally confirm our conclusions.

Pyrite will therefore not significantly contribute to the retardation of ^{129}I migration under the reducing conditions of a nuclear waste repository. Among other potential naturally-occurring sorbents for ^{129}I , natural organic matter which may be stable for geological storage seems to be the most promising candidate [35].

Conclusion

Batch experiments over a wide concentration and pH range under nearly anoxic conditions showed that pyrite cannot be considered as an effective scavenger towards radio-iodide in a radioactive waste repository environment. R_d values ranged between 5×10^{-4} and $1.7 \times 10^{-3} \text{ m}^3 \text{ kg}^{-1}$ at iodide concentrations $\leq 10^{-6} \text{ M}$. At an iodide concentration of 10^{-3} M , the amount of iodide sorbed was below the detection limit. Our results suggest that iodide uptake was related to the formation of Fe(III) oxide-like clusters at the pyrite surface due reactions with dissolved oxygen. Larger uptake values previously reported in the literature were probably due to surface oxidation prior to the start of the experiment. Oxidation processes are not expected under the anoxic conditions of an underground nuclear waste repository. Therefore, it is concluded that pyrite will not contribute significantly to the retardation of ^{129}I migration and to the reduction of calculated doses for performance assessments of deep radioactive waste storage. These results are consistent with the weak iodine retention measured in diffusion experiments with pyrite-containing clays.

Acknowledgments Valuable discussions with Dr. Dmitrii Kulik are greatly acknowledged. The authors wish also to thank Dr. Urs Eggenberger, and Christoph Wanner from the University of Bern, for BET measurements and for XRD assistance. The experienced support of Dr. Sousan Abolhassani-Dadras from Paul Scherrer Institute is greatly acknowledged. This work was partially funded by the Helmholtz Virtual Institute of “Advanced Solid-Aqueous Radiogeochemistry”.

References

1. Nagra (2002) Technical Report. NTB 02–05. Nagra, Wettingen, Switzerland
2. Nagra (2004) Technical Report. NTB 04–08. Nagra, Wettingen, Switzerland
3. Claret F, Lerouge C, Laurieux T, Bizi M, Conte T, Ghestem JP, Wille G, Sato T, Gaucher EC, Giffaut E, Toumassat C (2010) Natural iodine in a clay formation: Implications for iodine fate in geological disposals. *Geochim Cosmochim Acta* 74(1):16–29
4. Szanto Z, Svingor E, Molnar M, Palcsu L, Futo I, Szucs Z (2002) Diffusion of H-3, Tc-99, I-125, Cl-36 and Sr-85 in granite, concrete and bentonite. *J Radioanal Nucl Chem* 252(1):133–138
5. Weerasooriya R, Tobschall HJ (2005) Pyrite–water interactions: effects of pH and pFe on surface charge. *Colloids Surf A Physicochem Eng Asp* 264(1–3):68–74
6. Widler AM, Seward TM (2002) The adsorption of gold(I) hydrosulphide complexes by iron sulphide surfaces. *Geochim Cosmochim Acta* 66(3):383–402
7. Das DK, Pathak PN, Kumar S, Manchanda VK (2009) Sorption behavior of Am^{3+} on suspended pyrite. *J Radioanal Nucl Chem* 281(3):449–455
8. Borah D, Senapati K (2006) Adsorption of Cd(II) from aqueous solution onto pyrite. *Fuel* 85(12–13):1929–1934
9. Kosmulski M (2009) pH-dependent surface charging and points of zero charge IV. Update and new approach. *J Colloid Interface Sci* 337(2):439–448

10. Fuhrmann M, Bajt S, Schoonen MAA (1998) Sorption of iodine on minerals investigated by X-ray absorption near edge structure (XANES) and I-125 tracer sorption experiments. *Appl Geochem* 13(2):127–141
11. Strickert R, Friedman AM, Fried S (1980) The sorption of technetium and iodine radioisotopes by various minerals. *Nucl Technol* 49(2):253–266
12. Zhuang H, Zeng JS, Zhu LY (1988) Sorption of radionuclides technetium and iodine on minerals. *Radiochim Acta* 44–45: 143–145
13. Kaufhold S, Pohlmann-Lortz M, Dohrmann R, Nuesch R (2007) About the possible upgrade of bentonite with respect to iodide retention capacity. *Appl Clay Sci* 35(1–2):39–46
14. Naveau A, Monteil-Rivera F, Guillon E, Dumonceau J (2006) XPS and XAS studies of copper(II) sorbed onto a synthetic pyrite surface. *J Colloid Interface Sci* 303(1):25–31
15. Mell P, Megyeri J, Riess L, Mathe Z, Csicsak J, Lazar K (2006) Sorption of Co, Cs, Sr and I onto argillaceous rock as studied by radiotracers. *J Radioanal Nucl Chem* 268(2):405–410
16. Glaus MA, Muller W, Van Loon LR (2008) Diffusion of iodide and iodate through Opalinus Clay: monitoring of the redox state using an anion chromatographic technique. *Appl Geochem* 23(12):3612–3619
17. Tournassat C, Gaucher EC, Fattahi M, Grambow B (2007) On the mobility and potential retention of iodine in the Callovian–Oxfordian formation. *Phys Chem Earth* 32(8–14):539–551
18. Luther GW (1991) Pyrite synthesis via polysulfide compounds. *Geochim Cosmochim Acta* 55(10):2839–2849
19. Moses CO, Herman JS (1991) Pyrite oxidation at circumneutral pH. *Geochim Cosmochim Acta* 55(2):471–482
20. Imai H, Kawasaki M, Yamaguchi M, Takahashi M (1985) Mineralization and paragenesis of the Huanzala Mine, central Peru. *Econ Geol* 80(2):461–478
21. Lodders K, Klingelhofer G, Kremser DT (1998) Chloritoid inclusions in pyrite from Navajun, Spain. *Can Miner* 36:137–145
22. Elsetinow AR, Strongin DR, Borda M, Schoonen MAA (2001) Fundamental studies of the surface reactivity of pyrite. *Abstr Pap Am Chem Soc* 222:U488
23. Kandedgara A, Rorabacher DB (1999) Noncomplexing tertiary amines as “better” buffers covering the range of pH 3–11. Temperature dependence of their acid dissociation constants. *Anal Chem* 71(15):3140–3144
24. Hubner T, Will S, Leipertz A (1999) Determination of particle mass density distribution. *Part Part Syst Charact* 16(2):85–91
25. Bevington PR (1969) *Data reduction and error analysis for the physical sciences*. McGraw Hill Book Company, New York
26. Descostes M, Vitorge P, Beaucaire C (2004) Pyrite dissolution in acidic media. *Geochim Cosmochim Acta* 68(22):4559–4569
27. Williamson MA, Rimstidt JD (1994) The kinetics and electrochemical rate-determining step of aqueous pyrite oxidation. *Geochim Cosmochim Acta* 58(24):5443–5454
28. Wersin P, Curti E, Appelo CAJ (2004) Modelling bentonite–water interactions at high solid/liquid ratios: swelling and diffuse double layer effects. *Appl Clay Sci* 26(1–4):249–257
29. Lide DR (ed) *CRC handbook of chemistry and physics*, 90th edition (2009–2010). Maryland (USA) edn. CRC Press, Taylor and Francis Group, Boca Raton
30. Butler IB, Schoonen MAA, Rickard DT (1994) Removal of dissolved-oxygen from water—a comparison of 4 common techniques. *Talanta* 41(2):211–215
31. Hummel W, Berner U, Curti E, Pearson FJ, Thoenen T (2002) *Nagra/PSI chemical thermodynamic data base 01/01*. Universal Publishers, Parkland
32. Wagman DD, Evans WH, Parker VB, Schumm RH, Halow I, Bailey SM, Churney KL, Nuttall RL (1982) *The NBS tables of chemical thermodynamic properties—selected values for inorganic and C-1 and C-2 organic-substances in SI units*. *J Phys Chem Ref Data* 11:1–391
33. Rimstidt JD, Vaughan DJ (2003) Pyrite oxidation: a state-of-the-art assessment of the reaction mechanism. *Geochim Cosmochim Acta* 67(5):873–880
34. Schwertmann U (1991) Solubility and dissolution of iron-oxides. *Plant Soil* 130(1–2):1–25
35. Steinberg SM, Schmetz GT, Kimble G, Emerson DW, Turner MF, Rudin M (2008) Immobilization of fission iodine by reaction with insoluble natural organic matter. *J Radioanal Nucl Chem* 277(1): 175–183